

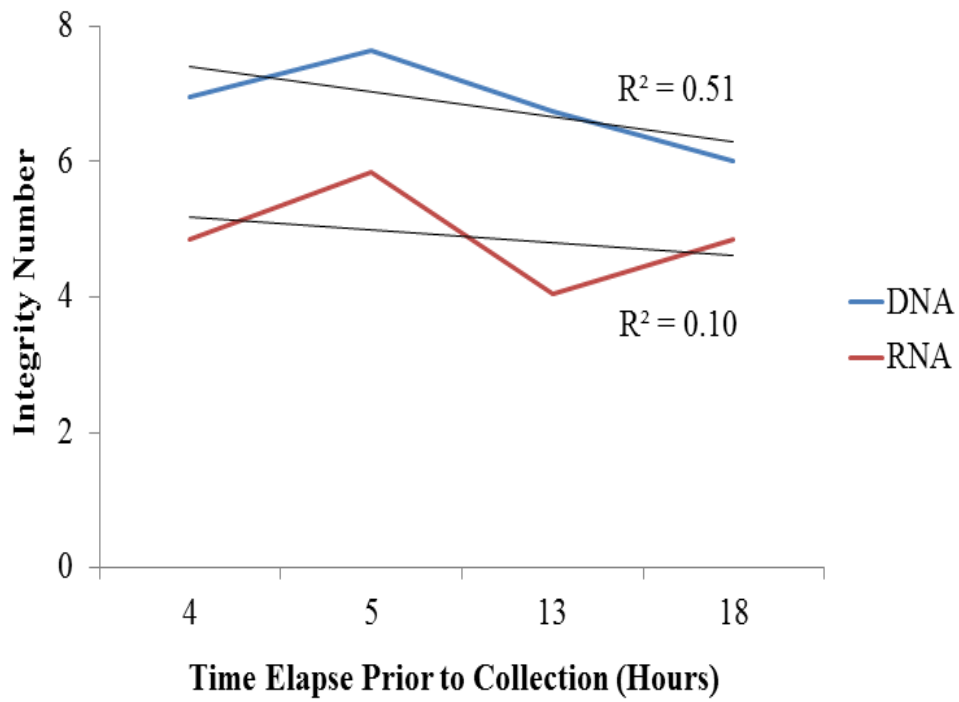
Supplemental Figures Legends

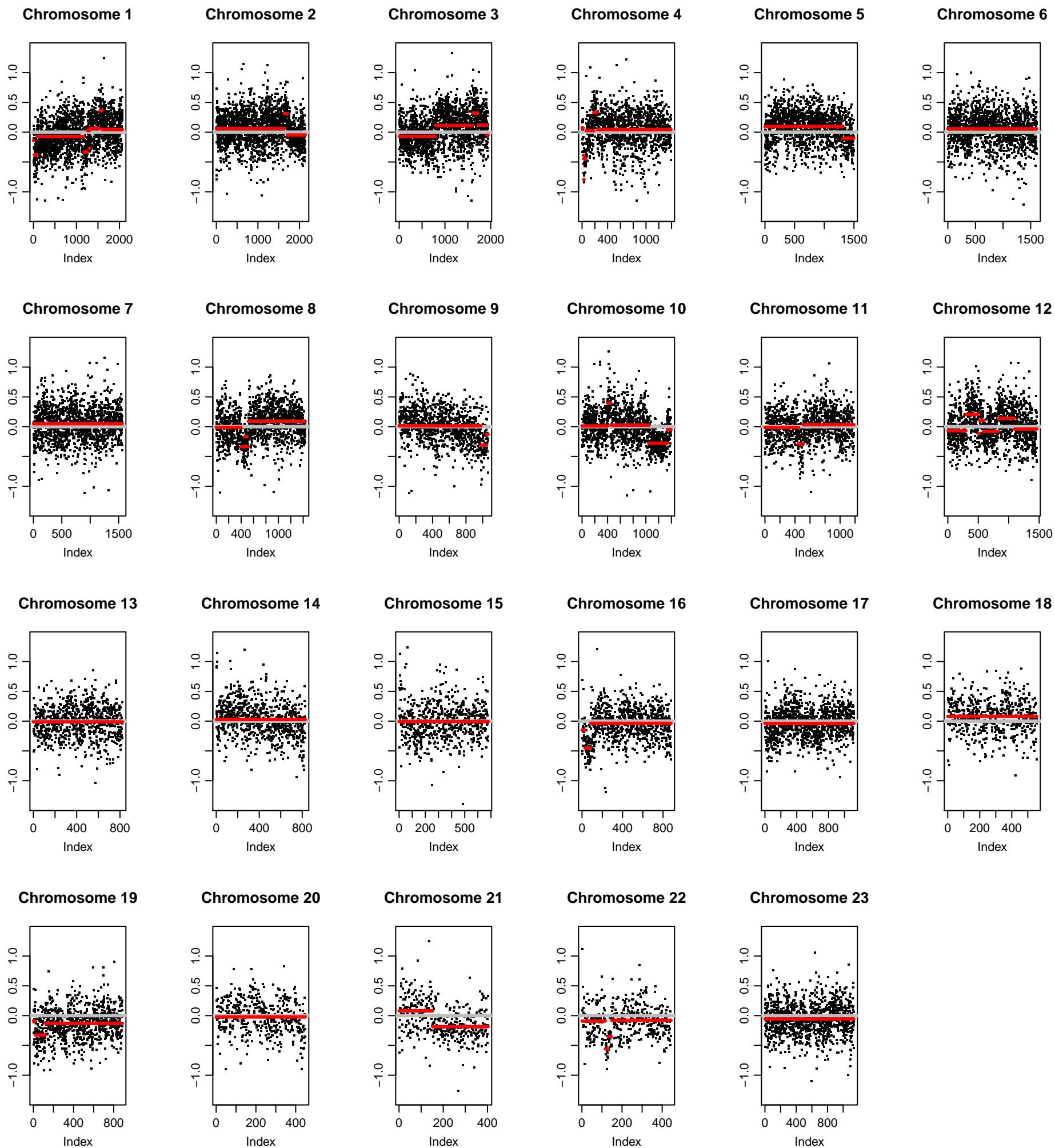
Supplemental Figure 1. The time in hours elapsed between death and tissue collection was plotted against average DNA or RNA integrity (DIN and RIN) score per rapid tissue donation case (N=4 cases).

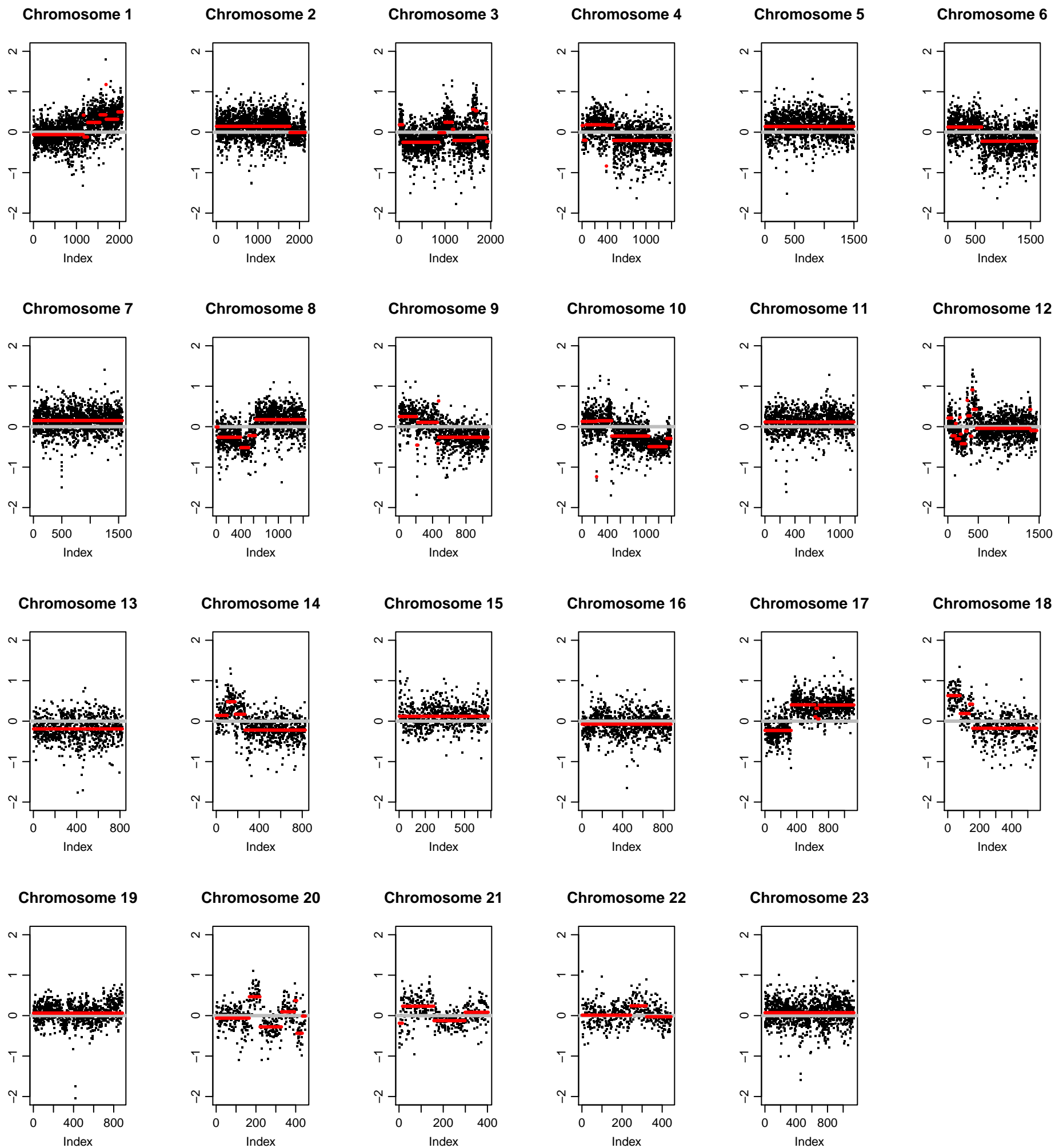
Supplemental Figure 2, A-E. Chromosome plots for Patient 1 (2A), Patient 3 (2B), Patient 4 (2C), Patient 6 (2D), and Patient 7 (2E) depict genetic changes at the chromosomal level by chromosome. For example, in patient 3, complex aneuploidy of chromosome 8q (including *MYC*), as well as focal deletions in chromosomal regions 4p16 (*FGFR3*) and 9q34, was identified in both tumor sites. In patient 4, broad level chromosomal changes were identified in all 3 sequenced lesions, including arm-level gains of chromosomes 3q, 5p, 8q, and 18q and arm-level losses of chromosomes 5q, 10, and 17p. In patient 6, the lymph node metastasis harbored several focal high-level amplifications in chromosome 12q15 (including *MDM2*) and chromosome 14q13 (near *NKX2-1*) that were not detected in the lung tumor sites.

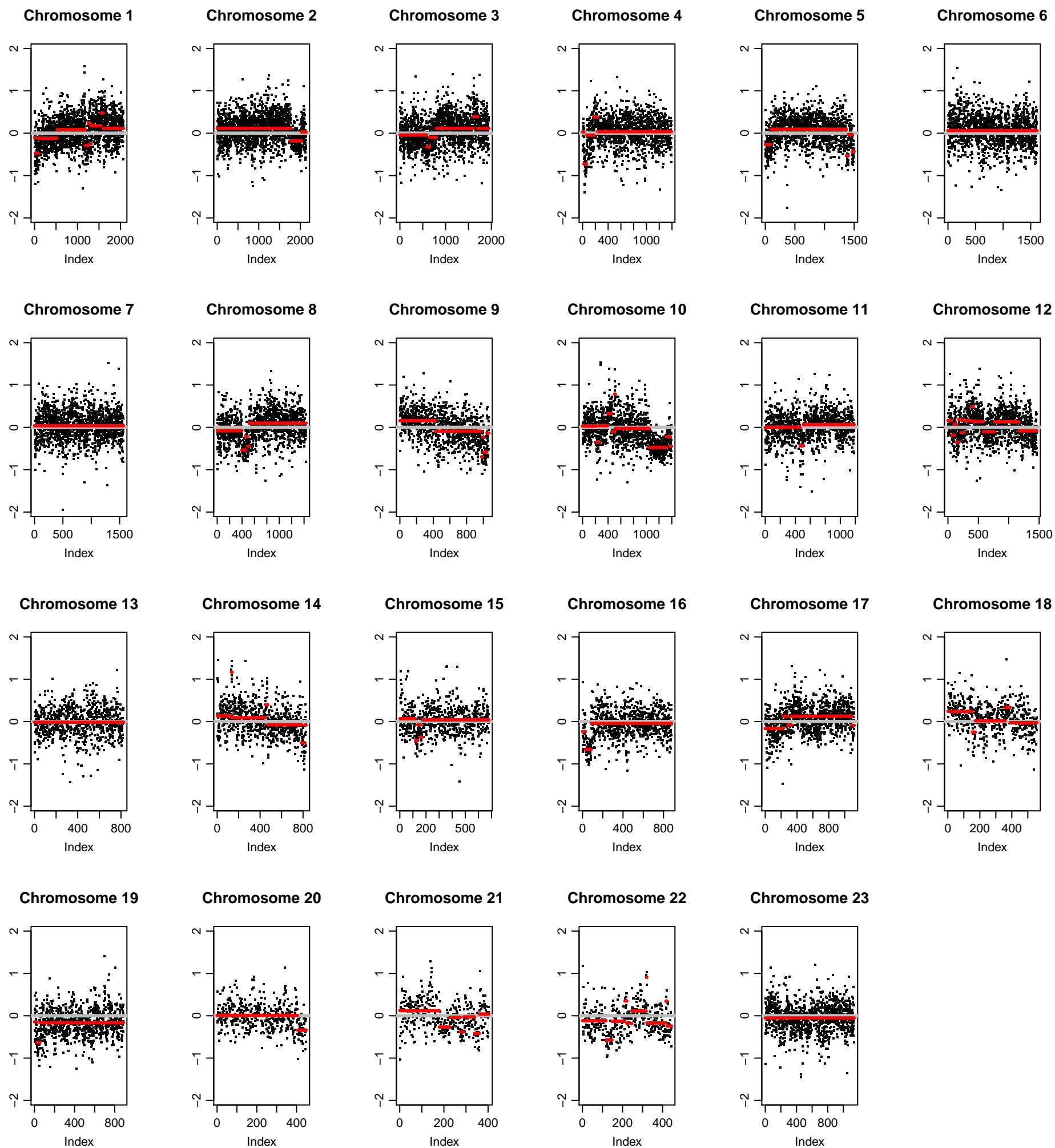
Supplemental Figure 3. Principle components analysis based on read counts from RNA-seq were used to assess the global similarity of RNA profiles by tumor site. Two liver metastatic lesions from patients 1 and 4 were more similar than the other lesions from the same patient, consistent with elevated levels of several liver-specific transcripts.

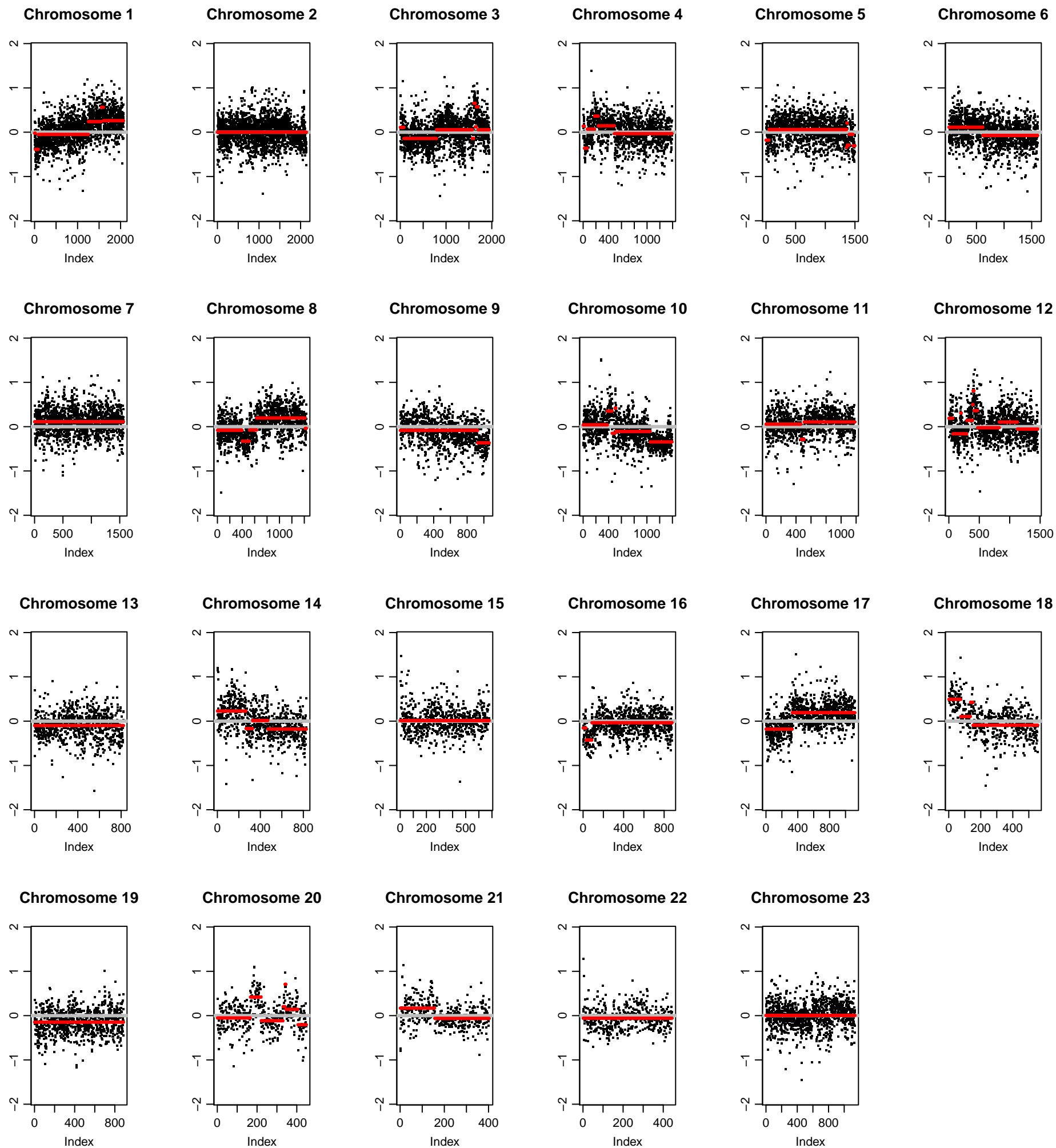
Supplemental Figure 1

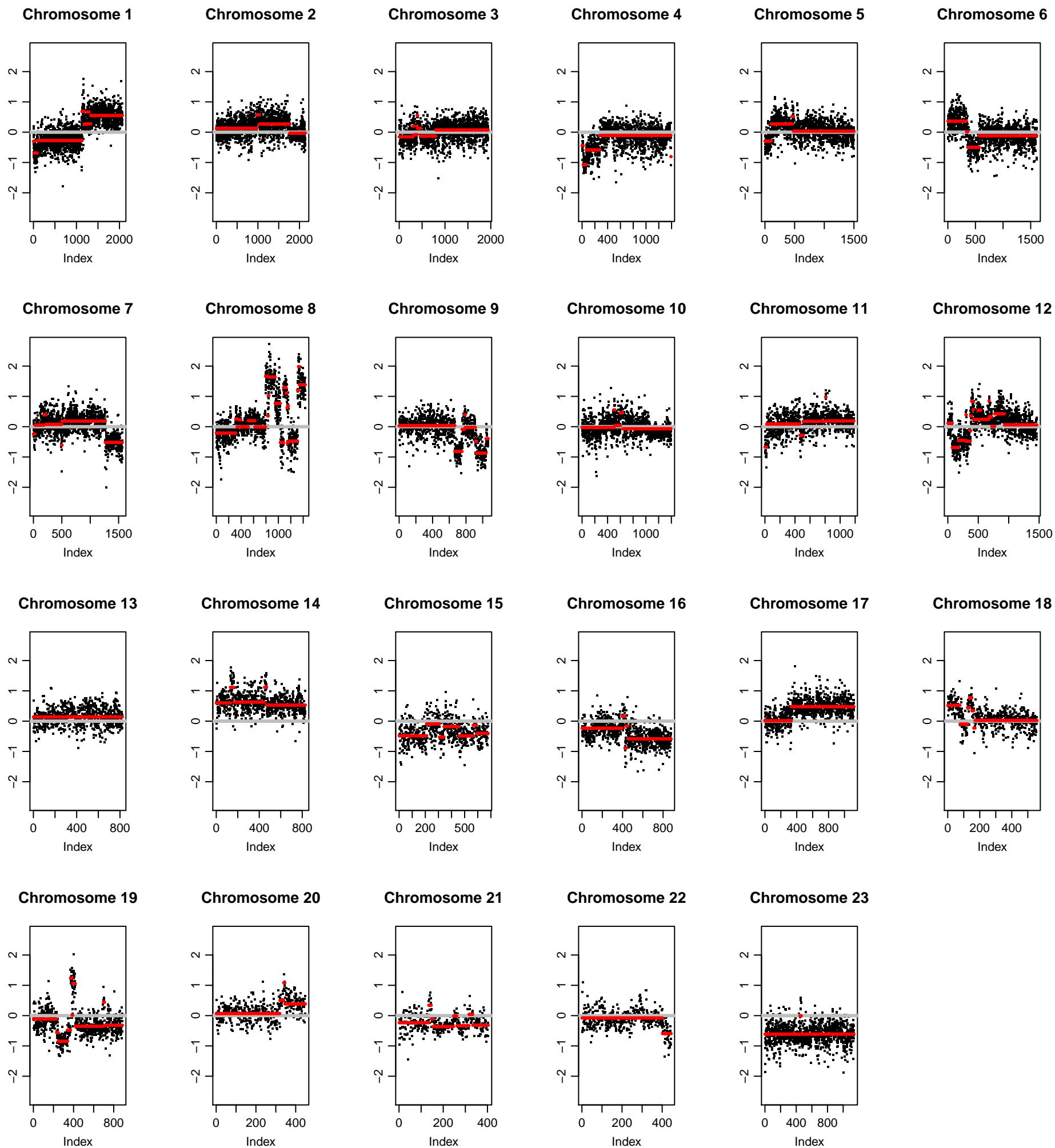


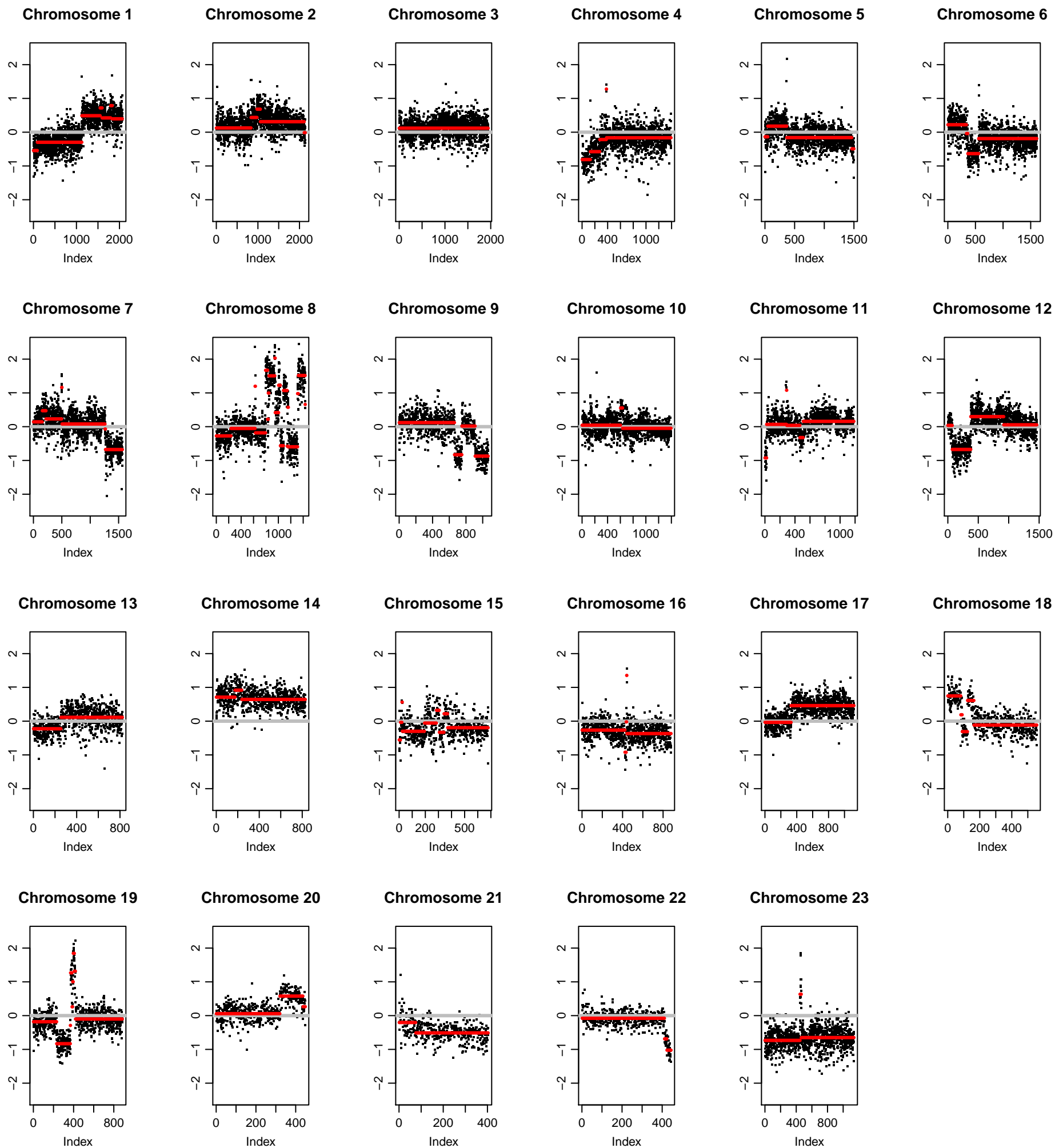


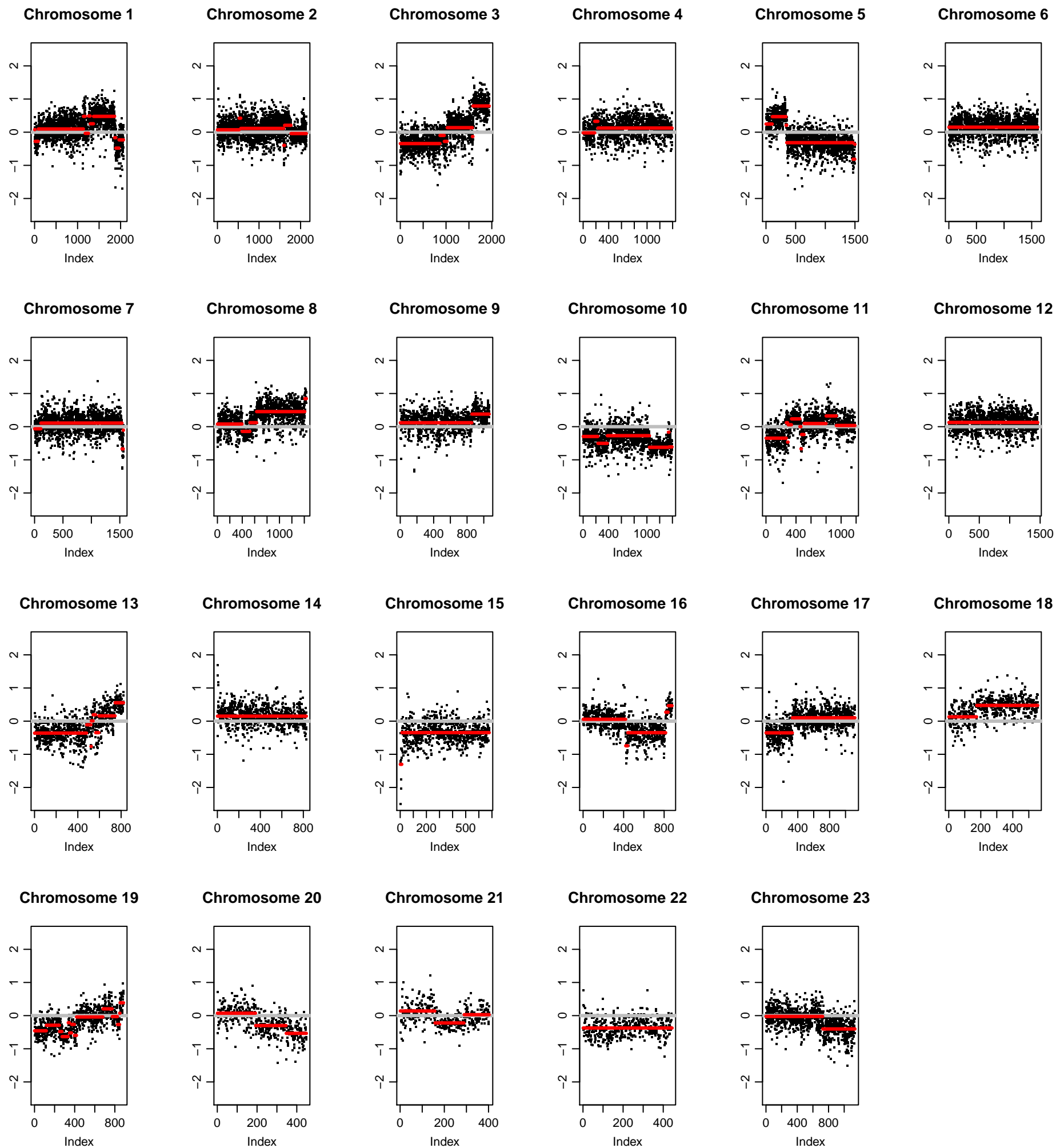


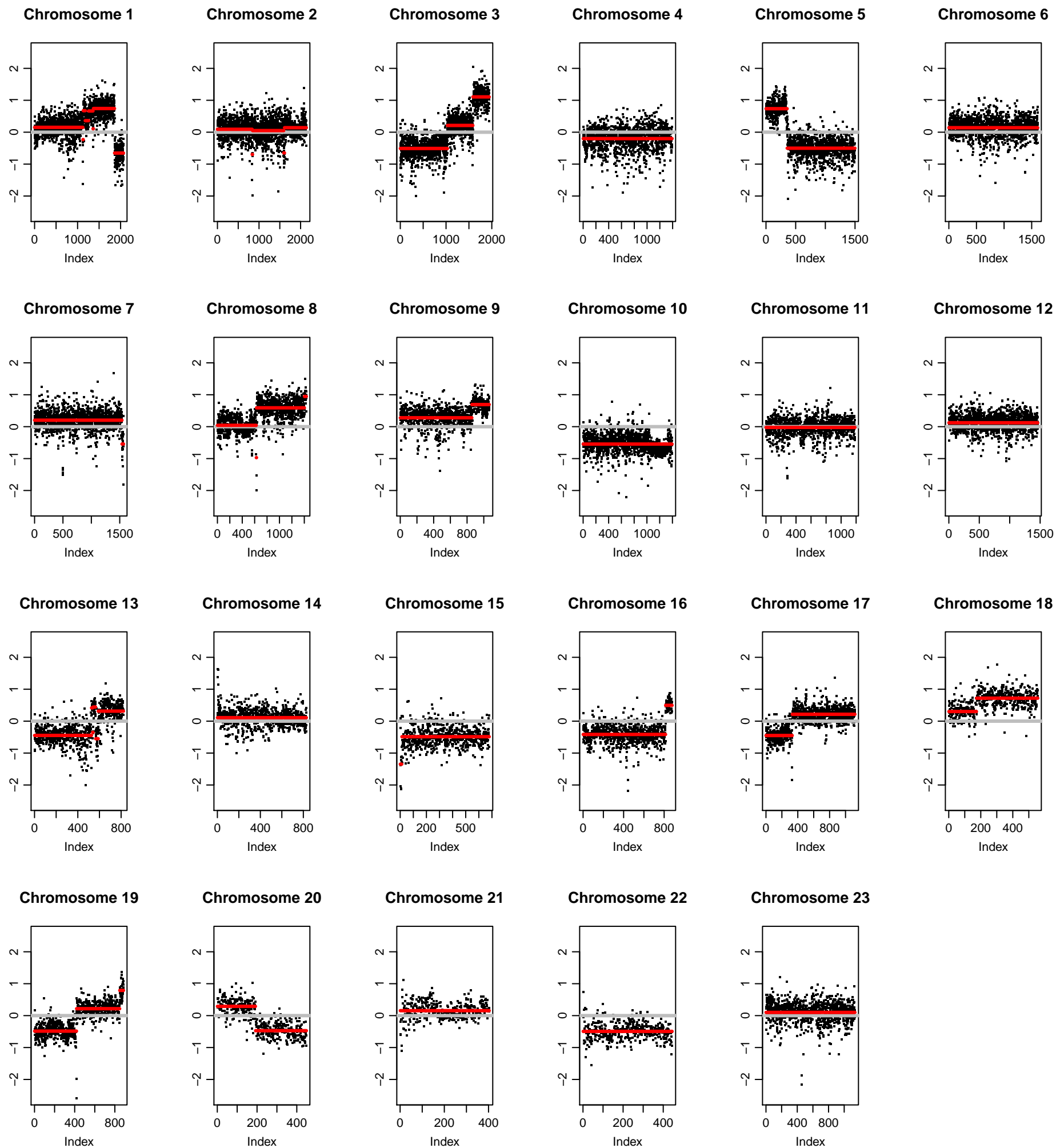


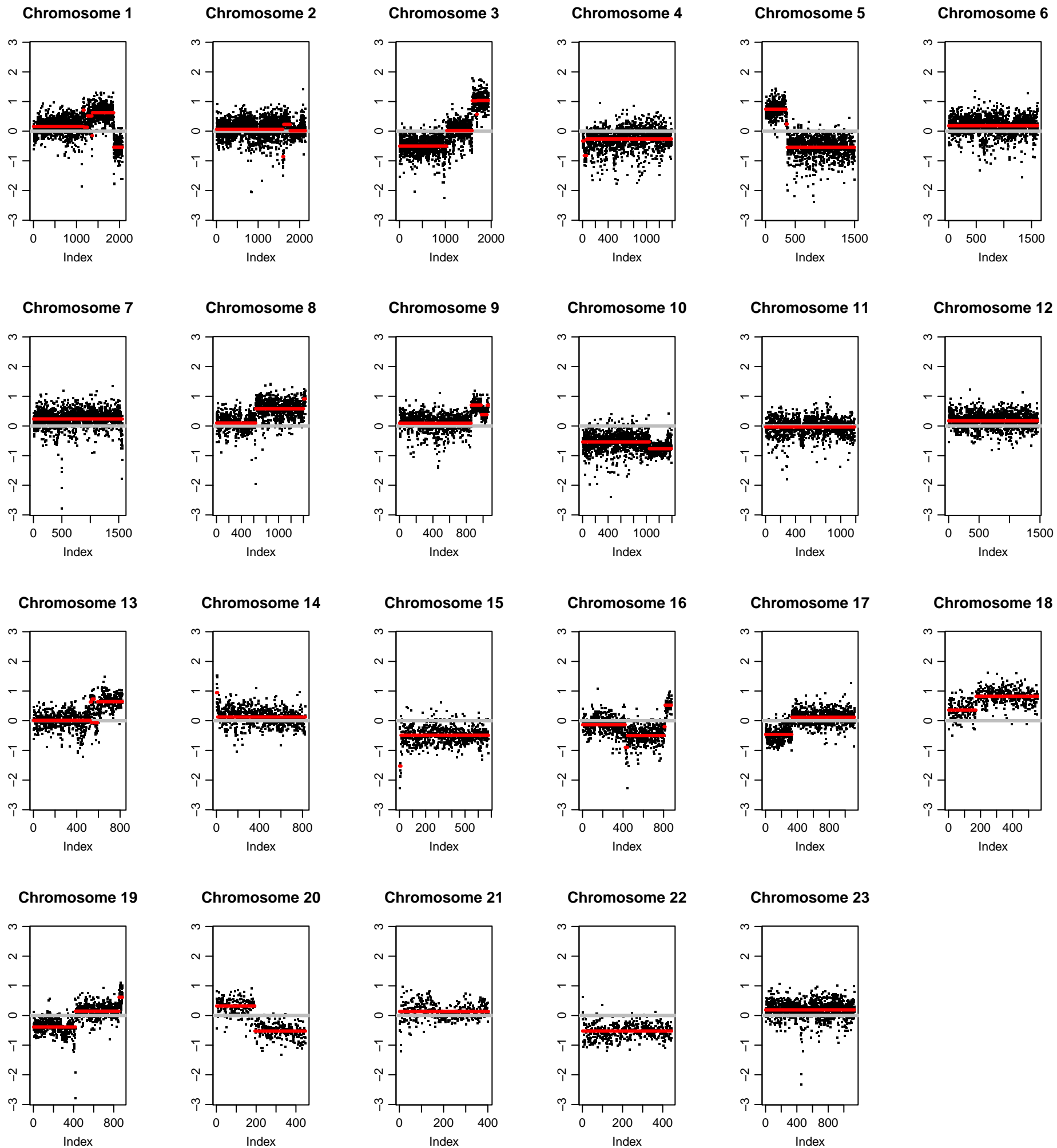






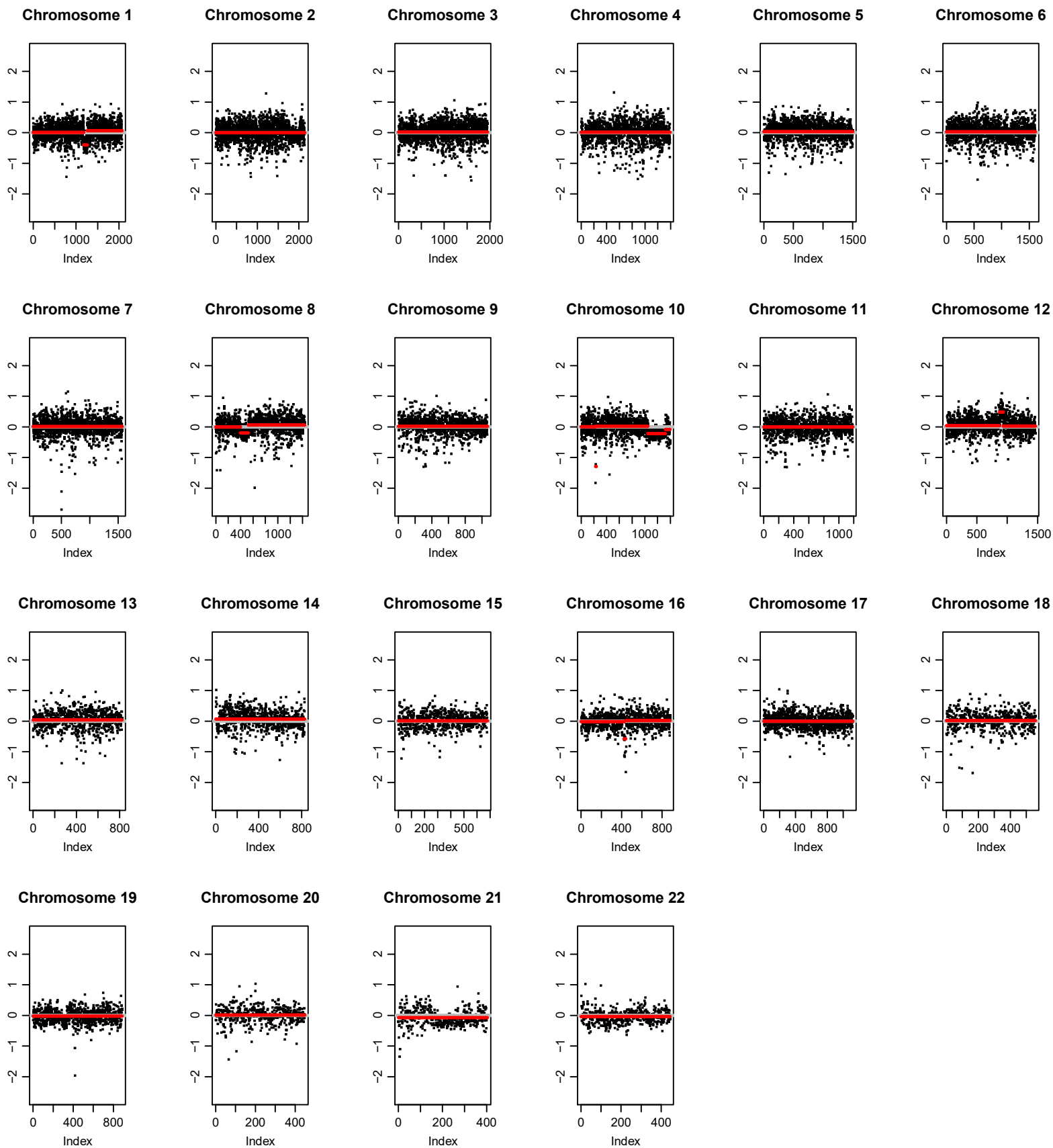






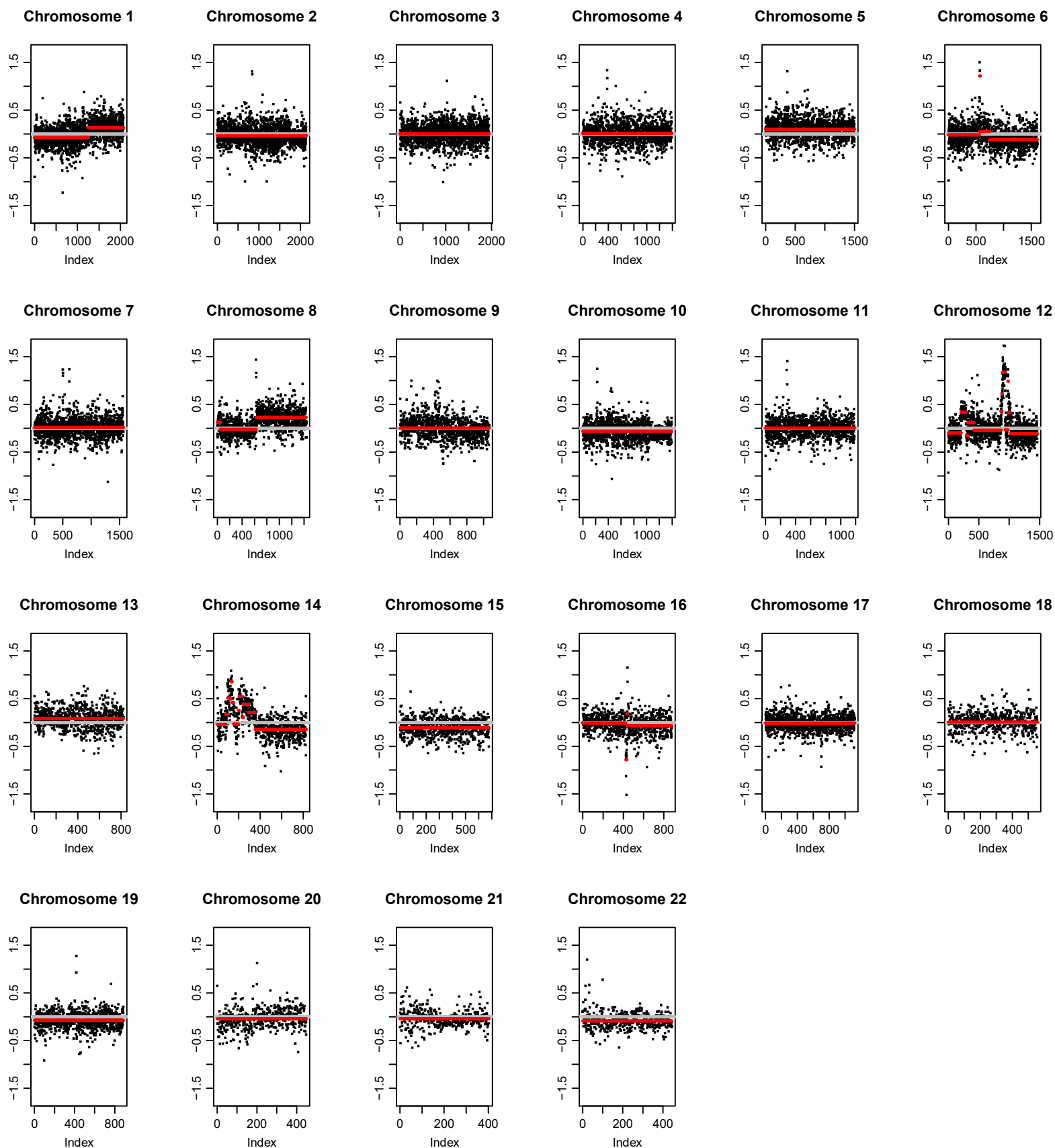
Supplemental Figure 2D (Patient 6: Left lower lung)

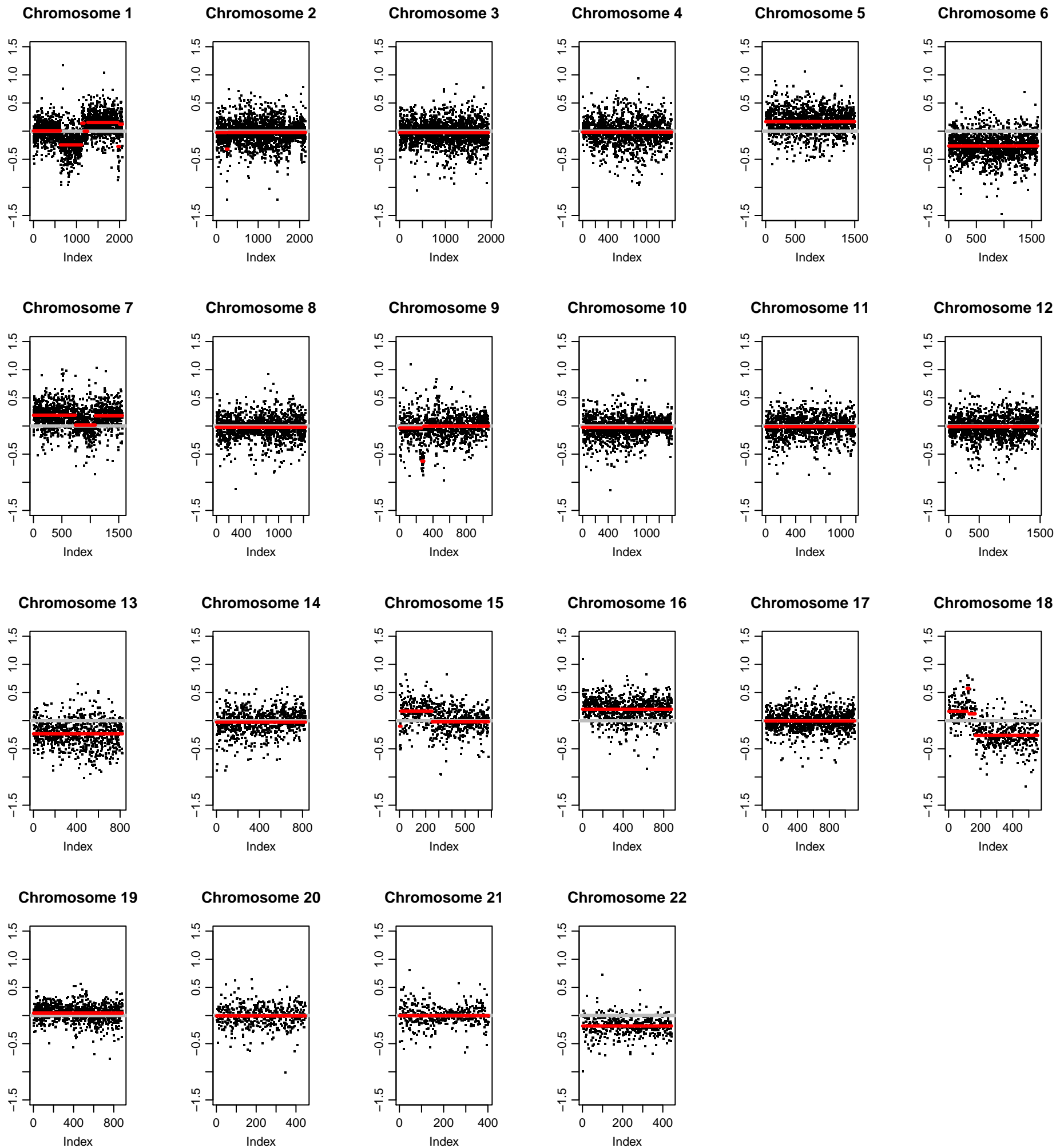
LIB.021184pc3.1

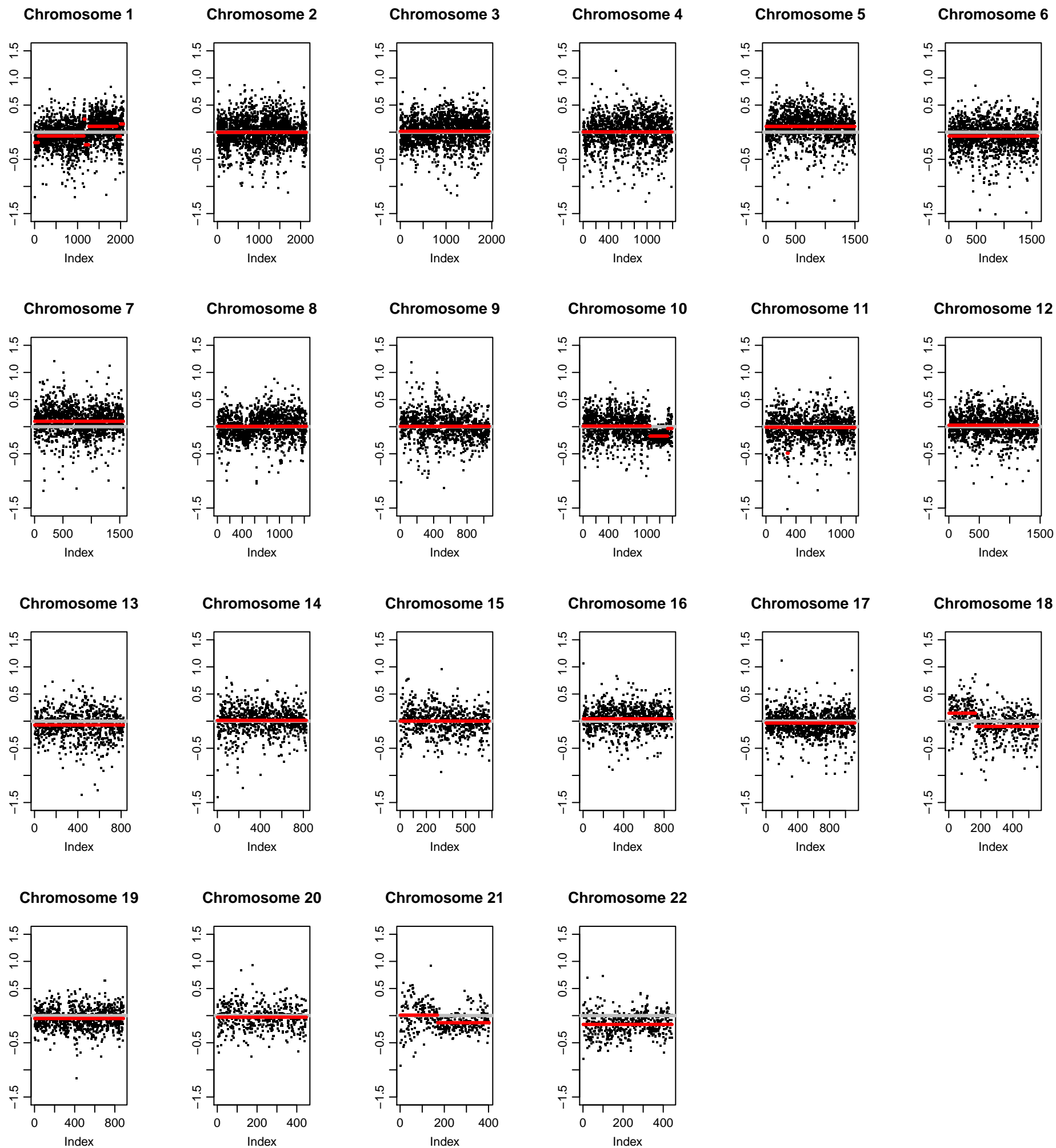


Supplemental Figure 2D (Patient 6: Lymph Node)

LIB.021178pc3.1







Liver-specific transcripts

